CMR Fundamental and Layered Systems Alex Bratkovsky, Chairman

# Optical and magnetic property of $LaMnO_3$

K. H. Ahn[a] and A. J. Millis
*Department of Physics and Astronomy, Rutgers University, Piscataway, New Jersey 08854*

A tight binding parameterization of the band structure, along with a mean field treatment of Hund, electron–electron, and electron–lattice couplings, is used to obtain the full optical conductivity tensor of $LaMnO_3$ as a function of temperature. We predict the magnetic phase transition causes striking changes in the functional form and magnitude of the optical absorption. Our results differ from those obtained by the local density-functional approximation techniques. Possible origins of the discrepancy are discussed. © *2000 American Institute of Physics.* [S0021-8979(00)53708-6]

## I. INTRODUCTION

During the last several years, a lot of attention has been focused on the colossal magnetoresistance manganese perovskites.[1] The low energy ($\hbar\omega<4$ eV) physics of these materials is believed to be governed by Mn$e_g$ electrons, which are coupled by a strong Hund's coupling, $J_H$, to Mn$t_{2g}$ symmetry ''core spins'' and also interact with each other and with lattice distortions. In this work, we show how the magnetic phase transition can change the magnitude and anisotropy of the optical conductivity of the manganites' insulating ''parent compound'' $LaMnO_3$. We obtain an effective Hamiltonian for the low energy degrees of freedom by fitting band theory calculations to a tight binding model and adding Coulomb interaction terms. We then determine its optical conductivity and show how the different features in the spectrum may be used to determine the interaction parameters. The material is a (0, 0, $\pi$) antiferromagnet at low temperatures, while a paramagnet at room temperature. The Hund's coupling therefore leads to a peak structure with a pronounced and strongly temperature-dependent anisotropy.

## II. TIGHT BINDING MODEL AND BAND STRUCTURE AT $T=0$ K

According to band theory calculations[2,3] the conduction band is derived mainly from Mn$e_g$ symmetry $d$ orbitals and is well separated from other bands. We find that the band structure appropriate to the ideal cubic $ABO_3$ perovskite structure may be well represented by the following tight binding model:

$$H_{\mathrm{KE}}+H_{\mu}=-\frac{1}{2}\sum_{\mathbf{i},\boldsymbol{\delta},a,b,\alpha} t_{\boldsymbol{\delta}}^{ab} d_{\mathbf{i}a\alpha}^{\dagger} d_{\mathbf{i}+\boldsymbol{\delta}b\alpha}+\mathrm{H.c.} - \boldsymbol{\mu}\sum_{\mathbf{i},a,\alpha} d_{\mathbf{i}a\alpha}^{\dagger} d_{\mathbf{i}a\alpha}. \tag{1}$$

Here $\mathbf{i}$ represents the coordinates of the Mn sites (which in the ideal structure are arranged in a simple cubic lattice), $a,b$ represent the two degenerate Mn$e_g$ orbitals on a site, $\delta(=\pm x,y,z)$ labels the nearest neighbors of a Mn site, $\alpha$ denotes the spin state, and $t_{\delta}^{ab}$ is the hopping amplitude between orbital $a$ on site $\mathbf{i}$ and $b$ on site $\mathbf{i}+\boldsymbol{\delta}$. We choose $|\psi_1\rangle=|3z^2-r^2\rangle$ and $|\psi_2\rangle=|x^2-y^2\rangle$ as the two linearly independent $e_g$ orbitals on a site. The hopping matrix $t_{\boldsymbol{\delta}}^{ab}$ has a special form: for hopping along the $z$ direction, it connects only the two $|3z^2-r^2\rangle$ states, thus $t_z^{\mathrm{ab}}=t_{-z}^{\mathrm{ab}}=t_0$ for $a=b=1$, and zero otherwise. The hopping matrices in the other bond directions are obtained by appropriate rotations.

We now turn to the electron-lattice coupling. Below 800 K, $LaMnO_3$ exists in a distorted form of the $ABO_3$ perovskite structure. The important distortion is a Jahn–Teller distortion, which lifts the degeneracy of the $e_g$ levels on a site. To represent this we define $u_{\mathbf{i}}^a$ as the displacement along the $a$ direction of an oxygen ion located between Mn ions at $\mathbf{i}$ and $\mathbf{i}+\hat{a}$, and we define $v_{\mathbf{i}}^a=u_{\mathbf{i}}^a-u_{\mathbf{i}-\hat{a}}^a$. The experimentally observed distortion has two components: a $Q_2$ type staggered distortion with wave vector ($\pi$, $\pi$, 0), and a $Q_3$ type uniform distortion. This distortion leads to a Jahn–Teller term of the form

$$H_{\mathrm{JT}}=-\lambda\sum_{\mathbf{i},\alpha}\begin{pmatrix} d_{1,\mathbf{i},\alpha}^{\dagger} \\ d_{2,\mathbf{i},\alpha}^{\dagger}\end{pmatrix}^{T}\begin{pmatrix} -\overline{v} & (-1)^{i_x+i_y}\overline{w} \\ (-1)^{i_x+i_y}\overline{w} & \overline{v}\end{pmatrix}\times\begin{pmatrix} d_{1,\mathbf{i},\alpha} \\ d_{2,\mathbf{i},\alpha}\end{pmatrix}, \tag{2}$$

where $\overline{w}$ and $\overline{v}$ are the amplitudes of the staggered ($Q_2$) and uniform ($Q_3$) distortion, respectively, defined by $\overline{v}=v_{i=0}^{z}-(v_{i=0}^{x}+v_{i=0}^{y})/2$, $\overline{w}=\sqrt{3}(v_{i=0}^{x}-v_{i=0}^{y})/2$. We next consider the Hund's coupling. At $T=0$ K, the magnetic structure is of a (0, 0, $\pi$) antiferromagnet, leading to

$$H_{\mathrm{Hund}}=J_H S_c\sum_{i,a}\{[1-(-1)^{i_z}]d_{\mathbf{i},a,\uparrow}^{\dagger}d_{\mathbf{i},a,\uparrow}+[1+(-1)^{i_z}]d_{\mathbf{i},a,\downarrow}^{\dagger}d_{\mathbf{i},a,\downarrow}\}. \tag{3}$$

The total Hamiltonian is so far the sum of the terms considered. By diagonalizing this matrix in $k$ space, we can find the energy levels and eigenstates.

[a]On leave from Department of Physics and Astronomy, The Johns Hopkins University, Baltimore, MD 21218.

 

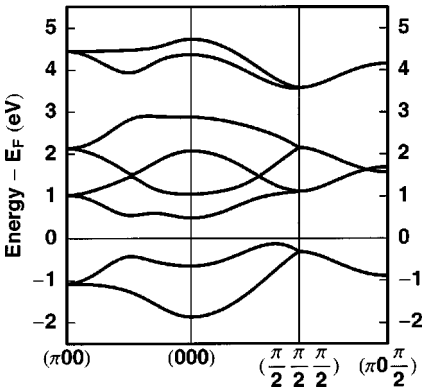


FIG. 1. Fitted $e_g$ band structure of $LaMnO_3$: $t_0=0.622$ eV, $2J_HS_c=2.47$ eV, $\lambda=1.38$ eV/Å, and $\mu=0.4$ eV. $(\pi,0,0)$, $(0,0,0)$, $(\pi/2,\pi/2,\pi/2)$, and $(\pi,0,\pi/2)$ points correspond to $M$, $\Gamma$, $R$, and $A$ points in Ref. 2, respectively.

Crudely speaking, the bands fall into four pairs, which may be understood by setting $t_0=0$ [as occurs at $(\pi/2,\pi/2,\pi/2)$]; in this case we have four separate energy levels on each site, which are $E_{1,2}=-\lambda\sqrt{\bar{v}^2+\bar{w}^2}$, $E_{3,4}=\lambda\sqrt{\bar{v}^2+\bar{w}^2}$, $E_{5,6}=2J_HS_c-\lambda\sqrt{\bar{v}^2+\bar{w}^2}$, and $E_{7,8}=2J_HS_c+\lambda\sqrt{\bar{v}^2+\bar{w}^2}$. To find the three parameter values of our model Hamiltonian, i.e., $t_0$, $\lambda$, and $J_HS_c$, we fit our band structure calculation to the LDA band calculation for the JT distorted $LaMnO_3$ by Satpathy *et al.*[2] at high symmetry points in reciprocal space. The standard deviation is $\approx 0.2$ eV. The determined parameter values are $t_0=0.622$ eV, $\lambda=1.38$ eV/Å, and $2J_HS_c=2.47$ eV. The fitted band structure is shown in Fig. 1.

## III. OPTICAL CONDUCTIVITY

### A. A-type antiferromagnetic phase at $T=0$ K

Optical conductivity per volume, $\sigma$, can be found from the eigenstates and energy levels found above. Using the standard linear response theory,[4] optical conductivity is given by

$$\sigma_p^{\lambda\nu}=-\frac{1}{i\omega N_{\mathrm{Mn}}a_0^3}\sum_n\frac{\langle 0|J_{p\lambda}^{\dagger}|n\rangle\langle n|J_{p\nu}|0\rangle}{\hbar\omega-(E_n-E_0)+i\epsilon}. \tag{4}$$

$a_0$ is the average Mn–Mn distance, $\epsilon$ is an infinitesimal, and $J_p$ is given by $\hat{\mathbf{J}}_p=-(iea_0/2\hbar)\Sigma_{\mathbf{i},\boldsymbol{\delta},a,b,\alpha}t_{\boldsymbol{\delta}}^{ab}\boldsymbol{\delta}(d_{\mathbf{i}a\alpha}^{\dagger}d_{\mathbf{i}+\boldsymbol{\delta}b\alpha}-\text{H.c.})$. Details of the calculations will be published elsewhere.

From crystallography studies in Ref. 5, $\bar{w}=0.488$ Å and $\bar{v}=0.174$ Å at $T=0$ K. Figures 2(a), 2(c), and 2(e) show the $T=0$ K optical conductivities $\sigma_{xx}$ and $\sigma_{zz}$ calculated for three sets of the coupling constant $\lambda$ and $J_HS_c$, with $t_0$ obtained in Sec. II. Figure 2(a) shows $\sigma_{xx}$ and $\sigma_{zz}$ for the case $2\lambda\sqrt{\bar{v}^2+\bar{w}^2}<2J_HS_c$. For $\sigma_{xx}$ (solid line), we see a large peak at the Jahn–Teller splitting, corresponding to motion within one plane. Note the jump in absorption at the gap edge, characteristic two-dimensional feature, a weak feature at $2J_HS_c$ and at the sum of the Jahn–Teller and Hund's splitting, corresponding to electron trajectories which overlap from one plane to the next. For $\sigma_{zz}$ (dotted line), alternating core spin direction along $\hat{z}$ direction results in the peaks at Hund energy and Hund+JT energy. Figure 2(c) shows the case of the Jahn–Teller coupling greater than Hund's coupling. In this case the Hund's feature appears strongly for both $\sigma_{xx}$ and $\sigma_{zz}$, whereas the Jahn–Teller feature is now almost completely absent in $\sigma_{zz}$. Figure 2 (e) show the results for a higher value of $J_HS_c$, which show the shift of the Hund's peak in $\sigma_{zz}$.

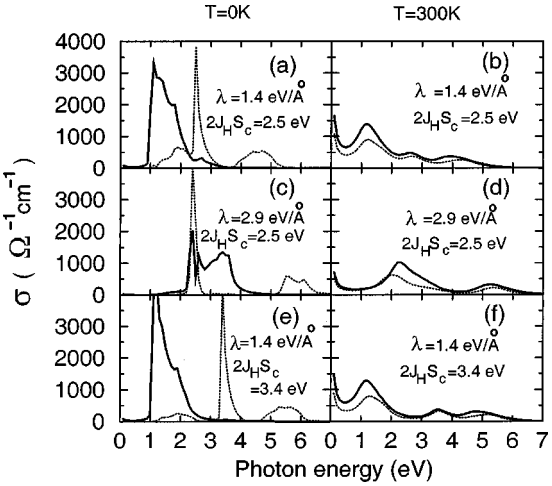


FIG. 2. Optical conductivities $\sigma_{xx}$ (solid lines) and $\sigma_{zz}$ (dotted lines) for $t_0=0.622$ eV without Coulomb repulsion ($U=0$).

### B. Paramagnetic phase at $T=300$ K

Since $T_N=140$ K for $LaMnO_3$, by room temperature it is reasonable to assume that the core spins are completely disordered. To describe the system at $T_N\ll T\ll T_{\mathrm{structure}}$ $(=800\text{ K})$, we develop the effective Hamiltonian in the following way. Instead of choosing spin basis along a fixed direction independent of sites, we choose $\Uparrow$ on site $\mathbf{i}$ as the direction of $e_g$ electron parallel to the core spin on site $\mathbf{i}$, and $\Downarrow$ as its opposite direction. Therefore, the Hund coupling energy is $H_{\mathrm{Hund}}=2J_HS_c\Sigma_{\mathbf{i},a}d_{\mathbf{i},a,\Downarrow}^{\dagger}d_{\mathbf{i},a,\Downarrow}$. $H_{\mu}$ and $H_{\mathrm{JT}}$ do not change their forms by the change of spin basis. If we define the angle between the core spin directions on site $\mathbf{i}$ and on site $\mathbf{i}+\boldsymbol{\delta}$ as $\theta_{\mathbf{i},\mathbf{i}+\boldsymbol{\delta}}$, the hopping amplitude is modified by a factor $\cos(\theta_{\mathbf{i},\mathbf{i}+\boldsymbol{\delta}}/2)$. Since $\theta_{\mathbf{i},\mathbf{i}+\boldsymbol{\delta}}$ will be completely random at $T\gg T_N$, by taking average $\langle\cos(\theta_{\mathbf{i},\mathbf{i}+\boldsymbol{\delta}}/2)\rangle=2/3$, we obtain

$$H_{\mathrm{KE}}^{\mathrm{eff}}=-\frac{1}{3}\sum_{\mathbf{i},\boldsymbol{\delta},a,b}t_{\boldsymbol{\delta}}^{ab}(d_{\mathbf{i}a\Uparrow}^{\dagger}d_{\mathbf{i}+\boldsymbol{\delta}b\Uparrow}+d_{\mathbf{i}a\Downarrow}^{\dagger}d_{\mathbf{i}+\boldsymbol{\delta}b\Downarrow}+d_{\mathbf{i}a\Uparrow}^{\dagger}d_{\mathbf{i}+\boldsymbol{\delta}b\Downarrow}+d_{\mathbf{i}a\Downarrow}^{\dagger}d_{\mathbf{i}+\boldsymbol{\delta}b\Uparrow}+\text{H.c.}). \tag{5}$$

To incorporate the level broadening due to spin fluctuation, we introduce a phenomenological broadening $\Gamma\approx t_o\sqrt{\langle\cos^2(\theta/2)\rangle-\langle\cos(\theta/2)\rangle^2}\approx 3t_o/\sqrt{2}$.

The general features of $\sigma_{xx}$ and $\sigma_{zz}$ at $T\gg T_N$ are these: Because we have random spin directions along both $x$ and $z$ directions, both $\sigma_{xx}$ and $\sigma_{zz}$ show JT, Hund, and JT+Hund peaks. Due to the anisotropy of the lattice distortion, we still expect anisotropy in the peak intensity. The broadening due to random spin directions makes the peaks smoother than the $T=0$ K case. Optical conductivities calculated for room temperature are shown in Figs. 2(b), 2(d), and 2(f), consistent with above explanation. For this calculation, we use the same $\lambda$, $t_o$, and $J_HS_c$ as in Figs. 2(a), 2(c), and 2(e), but we use

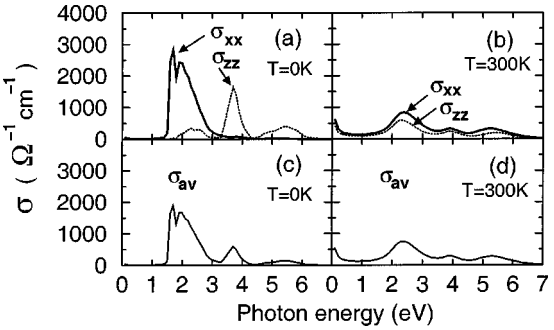


FIG. 3. Optical conductivities for $t_0=0.622$ eV, $2J_HS_c=2.47$ eV, $\lambda=1.38$ eV/Å, and $U=1.59$ eV.

the room temperature lattice parameters, which differ slightly from the 0 K lattice parameters. We obtain $\overline{w}=0.417$ Å and $\overline{v}=0.155$ Å from Ref. 5. The upturn of the optical conductivity at around zero frequency is an artifact of the crude consideration of the fluctuation in our model.

Recently, room temperature optical reflectivity spectra using a cleaved single crystal surface of $La_{1-x}Sr_xMnO_3$ have been measured by Takenaka *et al.*[6] Although it is referred to as a single crystal, we believe that the sample of $LaMnO_3$ is microtwined, and the measured quantity is $\sigma_{av}=2\sigma_{xx}/3+\sigma_{zz}/3$. In their results, the Jahn–Teller peak appears at around 2.5 eV. Similar results were obtained by Okimoto *et al.*[7] From Fig. 2(b), one sees that the observed lattice distortions would lead to the JT peak in $\sigma_{av}$ at 1.2 eV (lower than the experiment results), with spectral weight about twice the experiment results. We believe that the differences are mainly due to the Coulomb interaction whose effects we study in the next section.

## IV. COULOMB INTERACTION

We now add an on-site Hubbard-type Coulomb repulsion to our Hamiltonian:

$$H_{\text{Coulomb}}=\sum_{\mathbf{i}}\sum_{a\neq b}\sum_{\alpha\neq\beta}U\hat{n}_{\mathbf{i},\alpha,a}\hat{n}_{\mathbf{i}\beta,b}, \tag{6}$$

in which $\hat{n}$ is the density operator and $a$, $b$, $\alpha$, and $\beta$ represent the indices of the orbital basis picked out by the observed lattice distortion and the spin basis picked out by the magnetic ordering. We study this Hamiltonian in the Hartree–Fock approximation. We use $t_o$, $\lambda$, and $J_HS_c$ obtained previously and determine the values of $U$ by calculating optical conductivity at $T=300$ K and comparing with experimental JT peak position. For the JT peak at 2.5 eV in Takenaka *et al.*'s results, we obtain $U=1.6$ eV. The room temperature results are shown in Figs. 3(b) and 3(d), which shows that the calculated spectral weight is close to the observed spectral weight. With these determined values of $U$, we calculate $T=0$ K results shown in Figs. 3(a) and 3(c), which shows enhanced anisotropy and spectral weight.

## V. COMPARISON WITH LSDA CALCULATION OF OPTICAL CONDUCTIVITY

Terakura *et al.* have calculated the $T=0$ K optical conductivity using optical matrix elements and energies obtained from their LSDA band calculation.[8] Their conductivity is strikingly different from ours in two respects. First, the form is different: the sharp peaks we find are absent in their calculation. We suspect that the difference is due in large part to the $0.01\text{Ry}\approx 0.14$ eV level broadening employed in Ref. 8, and other bands we neglected in our model. A far more serious discrepancy is the difference in spectral weights. The area under the lowest conductivity peak in Ref. 8 is about a factor of 4 smaller than in our calculation. This difference seems not to be caused by a trivial error: in our calculation, the kinetic energies obtained from the direct integration of $\sigma$, agree with the results obtained from the Hellman–Feynman theorem.

We have examined the size of the possible error due to the following two approximations we have made: First, we have assumed that the hopping between Mn ions, which originates from Mn–O hopping, can be effectively represented without explicit consideration of O band. Second, we have used tight binding approximation. To study the first approximation, we consider a simple model of a 1-$d$ tight binding Mn–O chain, with O level explicitly considered. To estimate the error of the second approximation we consider a modified Kronig–Penney model, and find exact wave function and calculate optical conductivity. For both cases, we fit the band structure into Mn only tight binding model, and estimate the error. It indicates that when band fitting has about 5% error of total band width (similar to our case), the calculated spectral weight is reliable within 20% error. Therefore, within 20% error, we believe our calculated spectral weight is reliable.

## VI. CONCLUSION

First, the crucial prediction of the present model is the dramatic change in optical absorption with temperature. This change is a robust feature of the model, and comes from a dramatic shift in spectral weight caused by magnetic ordering. Second, we observe that the electron–lattice interaction by itself does not account for the magnitude of the gap or the spectral weight in the absorption spectrum. A Coulomb interaction $U\approx 1.6$ eV is also required. Finally, we note that a troubling discrepancy with the LDA optical conductivity calculation exists.

## ACKNOWLEDGMENTS

The authors thank H. Drew, S. Louie, O. Myrasov, and M. Quijada for helpful discussions, and Contract No. NSF-DMR-9705182 and the University of Maryland MRSEC for support.

[1] See, e.g., the articles in Philos. Trans. R. Soc. London, Ser. A **356**, 1469 (1998).
[2] S. Satpathy *et al.*, J. Appl. Phys. **79**, 4555 (1996).
[3] S. Satpathy *et al.*, Phys. Rev. Lett. **76**, 960 (1996); W. E. Pickett *et al.*, Phys. Rev. B **53**, 1146 (1996).
[4] E. Dagotto, Rev. Mod. Phys. **66**, 763 (1994).
[5] J. B. A. A. Ellemans *et al.*, J. Solid State Chem. **3**, 238 (1971).
[6] K. Takenaka, K. Iida, Y. Sawaki, S. Sugai, Y. Moritomo, and A. Nakamura (unpublished).
[7] Y. Okimoto *et al.*, Phys. Rev. B **55**, 4206 (1997).
[8] K. Terakura *et al.*, in *Colossal Magnetoresistive Oxides*, edited by Y. Tokura (Gordon and Breach, Tokyo, 1999).